

Article

Blind Spot Detection Radar System Design for Safe Driving of Smart Vehicles

Wantae Kim ¹, Heejin Yang ² and Jinhong Kim ^{3,*}

¹ Department of Information and Communication Engineering, Seoil University, Seoul 02192, Republic of Korea; wtkimseoil@naver.com

² Digital Edge Solutions Co., Ltd., Anyang 14056, Republic of Korea; hjang@digitaledge.co.kr

³ Department of Software, Paichai University, Daejeon 35345, Republic of Korea

* Correspondence: jinhkm@pcu.ac.kr; Tel.: +82-42-520-5071

Abstract: Recently, there has been extensive research and development in the field of smart cars, including technologies related to autonomous driving. Various industries are actively working towards creating efficient and safe self-driving cars. Sensor technologies are emerging to prevent traffic accidents and support safe driving in complex environments where human perception may be limited. One of the representative technologies being researched is the use of Frequency Modulated Continuous Wave (FMCW) radar. Automobile manufacturers are improving driving safety by equipping cars with Blind Spot Detection (BSD) radar systems that use FMCW technology. As the complexity of driving environments continues to grow, ongoing research is aimed at enhancing the accuracy and reliability of BSD radar technology for detecting blind spots in vehicles. This paper presents the signal processing and tracking algorithms that are the core technologies of the BSD radar, and the design for a BSD radar system. The designed radar system was installed on a vehicle to verify its performance in real-world road environments. The ultimate objective of this research is to design a BSD radar system with high accuracy and reliability in BSD detection using AI technology. In pursuit of this goal, this paper presents the hardware design of the BSD radar system, including antenna and modem designs.



Citation: Kim, W.; Yang, H.; Kim, J. Blind Spot Detection Radar System Design for Safe Driving of Smart Vehicles. *Appl. Sci.* **2023**, *13*, 6147. <https://doi.org/10.3390/app13106147>

Academic Editors: Andrea Prati, Junhong Park and Byung-Seo Kim

Received: 3 April 2023

Revised: 14 May 2023

Accepted: 15 May 2023

Published: 17 May 2023



Copyright: © 2023 by the authors. Licensee MDPI, Basel, Switzerland. This article is an open access article distributed under the terms and conditions of the Creative Commons Attribution (CC BY) license (<https://creativecommons.org/licenses/by/4.0/>).

1. Introduction

Various technologies are being developed to ensure the safe operation of vehicles, and one important element is the technology that detects the surroundings of the vehicle to ensure safety while driving or parking.

In recent years, there has been progress in the development of S-MaaS (Sustainable Mobility as a Service) [1] and research on autonomous driving. S-MaaS offers an alternative to unsustainable mobility based on personal vehicle use. To provide fully autonomous driving services for S-MaaS, it is essential to develop ITS (Intelligent Transport Systems), ICT (Information and Communication Technologies), TSM (Transport System Models), and DSS (Decision Support Systems) [2,3] together. To achieve autonomous driving, it is especially necessary to ensure safety through technology that can detect surrounding vehicles and respond to dangerous situations while driving. Furthermore, safety systems focused on drivers must be advanced to achieve autonomous driving [4].

Active safety systems are important technologies for ensuring the safe operation of vehicles, especially for smart cars. They can prevent or minimize accidents by alerting the driver to the situation in the front, back, and sides of the vehicle, using various sensors that detect the surrounding conditions. In the United States, Europe, and Japan, active safety systems and perception sensors are recognized as core automotive technologies, as the AEB (Autonomous Emergency Braking) [5] system has become mandatory. Active safety

systems use various technologies, including ACC (Advanced Cruise Control) [6], which uses radar and camera sensors to maintain a safe distance from the vehicle in front; FCW (Forward Collision Warning) [7], which uses radar sensors to detect a possible collision with a vehicle or obstacle in front of the car and alerts the driver; LCA (Lane Change Assistant) [8], which uses radar sensors to monitor the blind spots and alerts the driver if there is a potential collision when changing lanes; and RCTA (Rear Cross Traffic Alert) [9], which uses rear radar sensors to detect other vehicles crossing behind the vehicle and alerts the driver while controlling the brakes. To design active safety systems, it is crucial to detect blind spots around the vehicle. The BSD radar is a system that alerts the driver when another vehicle approaches the blind spot of the vehicle. It quickly distinguishes clutter and vehicles in proximity and provides this information to the driver. Therefore, it can be considered a key technology in designing active safety systems.

Reference [1] describes the components and essential technologies of S-MaaS for a future transportation system. It also presents the TSM for evaluating the contribution of transportation infrastructure and services to sustainability. References [2,3] provide evidence for the feasibility of S-MaaS through ICT, TSM, DSS, and ITS technologies. Reference [4] explains various technologies for autonomous driving. To ensure accurate detection of the surrounding situation while driving, this paper focuses on designing a BSD radar system as a technology related to S-MaaS. The critical technologies for designing the BSD radar include signal processing [10] and tracking technology [11].

In particular, the road environment requires tracking of multiple targets. BSD radar is a technology that interprets Range, Velocity, and Angle through the received signal when the transmitted signal collides with an object. References [12,13] explain the FMCW radar principle and algorithm that can detect objects by continuously transmitting signals and reflecting signals. References [14,15] explain the pre-existing technology for detecting stationary and moving targets, which is a fundamental function of the BSD radar system. To verify the signal forms in the time domain and the frequency domain for interpreting the equations and signals presented in the basic principles for designing the system, a simulation was performed using MATLAB TOOL with reference to [16,17], and the basic principles were verified. Reference [18] presents a detection method based on 2D FFT, which is similar to the technique used in this paper. However, this technology is for pedestrian detection, not for automotive applications. Nonetheless, the detection principle is similar. References [19–21] present multidimensional FFT for signal acquisition in radar sensors and provide performance evaluations for FFT usage. The utilization of both 2D FFT and multidimensional FFT techniques are referenced in this paper. References [22,23] serve as standardization documents for the design of a BSD radar system in this paper. They provide guidance for designing the system, outlining the requirements for performance evaluation and test scenarios. The BSD system presented in this paper was designed to meet all the requirements specified in [22,23].

The BSD radar system using FMCW continuously emits signals while driving, and the emitted signals bounce off nearby objects and return to the vehicle. This technology can detect the distance, angle, direction, and speed of the target vehicle, calculate the risk of collision with the vehicle, evaluate the driving situation, and inform the driver to ensure the safety of driving a car. The key technologies involved in designing the BSD radar system are signal processing technology, which detects the surrounding situation by analyzing the reflected signals after transmitting a signal [10], tracking algorithms for detecting the surrounding situation of the vehicle [11], and procedures for tracking target vehicles in the surrounding environment. This paper presents a tracking algorithm for designing a BSD radar system, while explaining the principles of FMCW radar technology and signal types. Additionally, this paper presents the target tracking procedure and target filter to design an accurate tracking system and explains the system design. Finally, the radar system that was developed is installed in a vehicle to evaluate the system's performance in a driving environment.

2. FMCW Radar Principle

The BSD radar system is designed using FMCW radar, which is capable of measuring Range (R), Velocity (V), and Angle (A). The principle of FMCW radar is to determine the R, V, and A of surrounding objects by analyzing the signal transmitted by the radar's transmitter and the signal reflected by surrounding objects and received by the radar's receiver [12,13]. The difference between the received signal and the transmitted signal is known as the beat frequency.

The BSD radar system considers two main situations to analyze the accurate R, V, and A of the surrounding targets. The first situation is a stationary target, and the second situation is a moving target. Stationary targets can be further classified into two categories: Single Stationary Target and Multiple Stationary Targets. Moving targets can also be classified into two categories: Single Moving Target and Multiple Moving Targets. Figure 1 illustrates the stationary target of the FMCW radar.

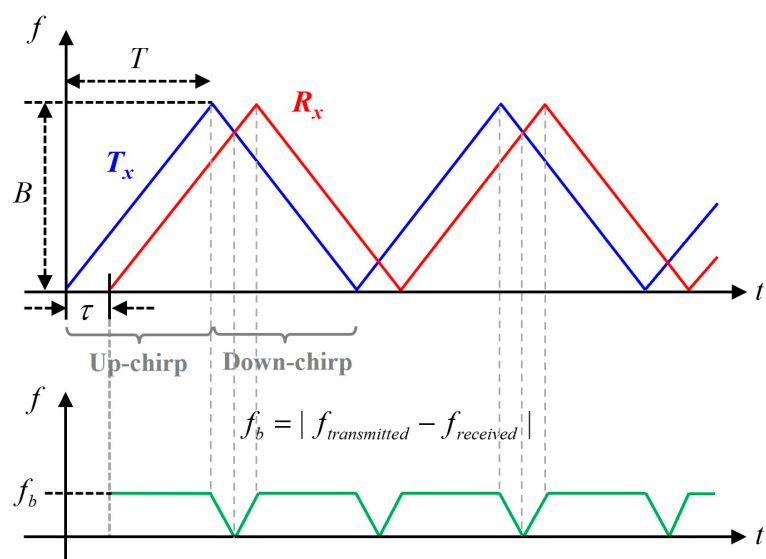


Figure 1. Beat Frequency for Stationary Target.

In Figure 1, the transmitted (Tx) signal from the system collides with the surrounding targets and the reflected signal is defined as the received (Rx) signal that enters the radar system. τ defines the time difference between the Tx and Rx signals, while B defines the frequency bandwidth. T is the sweet time, which defines the time for the amplitude to increase from the minimum value to the maximum value. Up-chirp defines the time for the amplitude of the signal to increase, while down-chirp defines the time for the amplitude of the signal to decrease. f_b is the beat frequency, which defines the frequency difference between the Tx and Rx signals. The FMCW radar system analyzes the R, V, and A of the surrounding targets with respect to the moving vehicle by using the beat frequency. As Figure 1 shows a stationary target, a time difference occurs between the Tx and Rx signals, but the bandwidth is the same between the two signals because the target is stationary. Therefore, in Figure 1, the analysis of beat frequency and range is an important factor.

In Figure 1, the equation for analyzing the beat frequency is shown as Equation (1):

$$\left\{ \frac{f_b}{\tau} = \frac{B}{T} \right\} \Rightarrow f_b = \tau \cdot \frac{B}{T} = \frac{2R}{C} \cdot \frac{B}{T}, \quad \begin{cases} B = \text{bandwidth [Hz]} \\ T = \text{sweep time [sec]} \\ R = \text{target range [m]} \\ \tau = \text{time delay [sec]} \\ c = 3e8 \left[\frac{\text{m}}{\text{s}} \right] \end{cases} \quad (1)$$

In the analysis of beat frequency, $2R$ is defined considering the round-trip distance to the target, where C represents the transmission speed of the signal, defined as the speed of light.

The equation for analyzing Range (R) in a stationary target is shown as Equation (2):

$$R = \frac{cTf_b}{2B} R_{max} = \frac{cTf_{b,max}}{2B} \Rightarrow R_{limit} = \frac{cT}{2}, (f_{b,max} = B) \quad (2)$$

In Equation (2), the actual maximum time difference (τ) is commonly defined as $0.1 \times T$. When considering a stationary target, the relative speed is zero. Thus, the equation $B = f_b$ is applicable. The parameter R can be defined using Equation (2). Figure 2 defines a moving target of the FMCW radar. There is a time difference between the beat frequencies of the Tx signal and the Rx signal, and a bandwidth difference occurs due to the movement of the target. In the presence of a moving target, the received signal experiences a shift due to the Doppler effect, which can be quantified by the Doppler frequency.

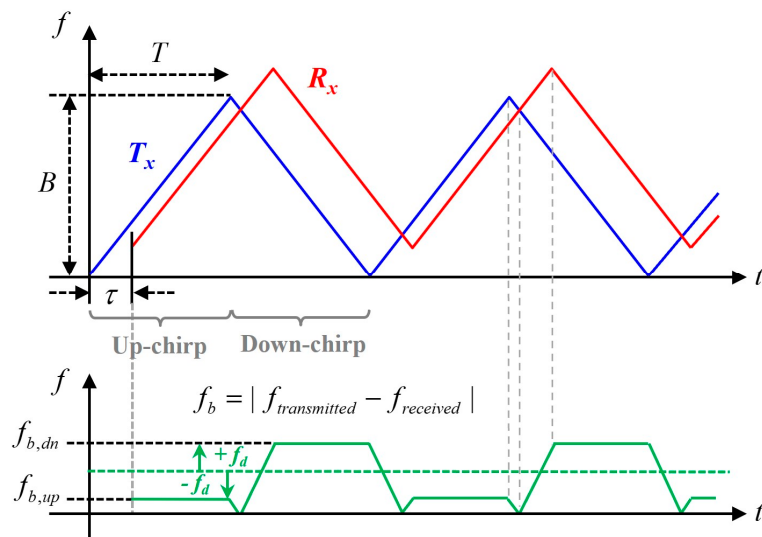


Figure 2. Beat Frequency for Moving Target.

The change in bandwidth is defined by the height on the frequency axis. The slope variation of the chirp signal, which increases the starting frequency for a certain period, is used to define the velocity.

To interpret the chirp signal in Figure 2, the beat frequency of the up-chirp and down-chirp is given by Equation (3):

$$f_{b,up} = \tau \cdot \frac{B}{T} - \frac{2v}{\lambda} = \frac{2RB}{cT} - f_d \quad (3)$$

$$f_{b,dn} = \tau \cdot \frac{B}{T} + \frac{2v}{\lambda} = \frac{2RB}{cT} + f_d, \begin{cases} f_d = \text{Doppler frequency [Hz]} \\ \lambda = \text{wavelenght [m]} \\ v = \text{target vwlocity [m/s]} \end{cases} \quad (4)$$

In a moving target environment, Range can be defined by Equation (5), and Velocity can be defined by Equation (6); additionally, the wavelength for interpreting the velocity can be defined by Equation (7):

$$R = \frac{cT}{4B} (f_{b,up} + f_{b,dn}) \quad (5)$$

$$v = \frac{\lambda}{4} (f_{b,up} - f_{b,dn}) \quad (6)$$

$$\lambda = \frac{c}{f_c} \quad (7)$$

In the design of a BSD radar system, the fundamental FMCW principle has been explained using Figures 1 and 2, and Equations (1)–(7). This paper provides a more detailed explanation of the fundamental principle of the FMCW radar signal used in the designed system. After setting arbitrary parameters for the Multiple Stationary Targets Case [14] and Multiple Moving Targets Case [15], by using MATLAB simulation tools [16,17], this paper examines the form of the beat frequency based on the Tx signal in the time domain and the form of the signal's spectrum in the frequency domain. The results are presented below. Table 1 shows the arbitrary parameters used to represent Multiple Stationary Targets, while Table 2 shows the arbitrary parameters used to represent Multiple Moving Targets. Three targets were set, and the Time Delay, Doppler Frequency, Amplitude, and Beat Frequency for the simulation were defined in each table.

Table 1. Parameters for Multiple Stationary Targets.

Target	Parameter	Value	Unit	Beat Frequency (Cal.)
Target 1	Time Delay (τ)	0.1	Sec	$f_{b,up} = \tau(B/T) + f_d = 5 \text{ [Hz]}$
	Doppler Freq. (f_d)	0	Hz	$f_{b,dn} = \tau(B/T) - f_d = 5 \text{ [Hz]}$
	Amplitude	1	Volt	
Target 2	Time Delay (τ)	0.2	Sec	$f_{b,up} = \tau(B/T) + f_d = 10 \text{ [Hz]}$
	Doppler Freq. (f_d)	0	Hz	$f_{b,dn} = \tau(B/T) - f_d = 10 \text{ [Hz]}$
	Amplitude	0.5	Volt	
Target 3	Time Delay (τ)	0.4	Sec	$f_{b,up} = \tau(B/T) + f_d = 20 \text{ [Hz]}$
	Doppler Freq. (f_d)	0	Hz	$f_{b,dn} = \tau(B/T) - f_d = 20 \text{ [Hz]}$
	Amplitude	0.3	Volt	

Table 2. Parameters for Multiple Moving Targets.

Target	Parameter	Value	Unit	Beat Frequency (Cal.)
Target 1	Time Delay (τ)	0.1	Sec	$f_{b,up} = \tau(B/T) + f_d = 4 \text{ [Hz]}$
	Doppler Freq. (f_d)	1	Hz	$f_{b,dn} = \tau(B/T) - f_d = 6 \text{ [Hz]}$
	Amplitude	1	Volt	
Target 2	Time Delay (τ)	0.2	Sec	$f_{b,up} = \tau(B/T) + f_d = 7 \text{ [Hz]}$
	Doppler Freq. (f_d)	3	Hz	$f_{b,dn} = \tau(B/T) - f_d = 13 \text{ [Hz]}$
	Amplitude	0.5	Volt	
Target 3	Time Delay (τ)	0.4	Sec	$f_{b,up} = \tau(B/T) + f_d = 15 \text{ [Hz]}$
	Doppler Freq. (f_d)	5	Hz	$f_{b,dn} = \tau(B/T) - f_d = 25 \text{ [Hz]}$
	Amplitude	0.3	Volt	

Figure 3 shows the simulation results for multiple stationary targets, assuming the presence of three targets. As all three targets are stationary, the frequencies of $f_{b,up}$ and $f_{b,dn}$ are identical. The characteristics of the beat frequency can be observed in the frequency domain, with frequency spectra appearing at the positions of 5 [Hz], 10 [Hz], and 20 [Hz] defined in Table 1.

Figure 4 shows the simulation results for multiple moving targets, assuming the presence of three targets. Since these targets are in motion, $f_{b,up}$ and $f_{b,dn}$ have different frequencies. In the frequency domain, the characteristics of $f_{b,up}$ of Targets 1, 2, and 3 can be observed, with frequency spectra appearing at 4 [Hz], 7 [Hz], and 15 [Hz] as defined in Table 2. Likewise, the characteristics of $f_{b,dn}$ can be observed with spectra appearing at 6 [Hz], 13 [Hz], and 25 [Hz]. Therefore, the equations proposed in this paper for the design of FWCM can be validated.

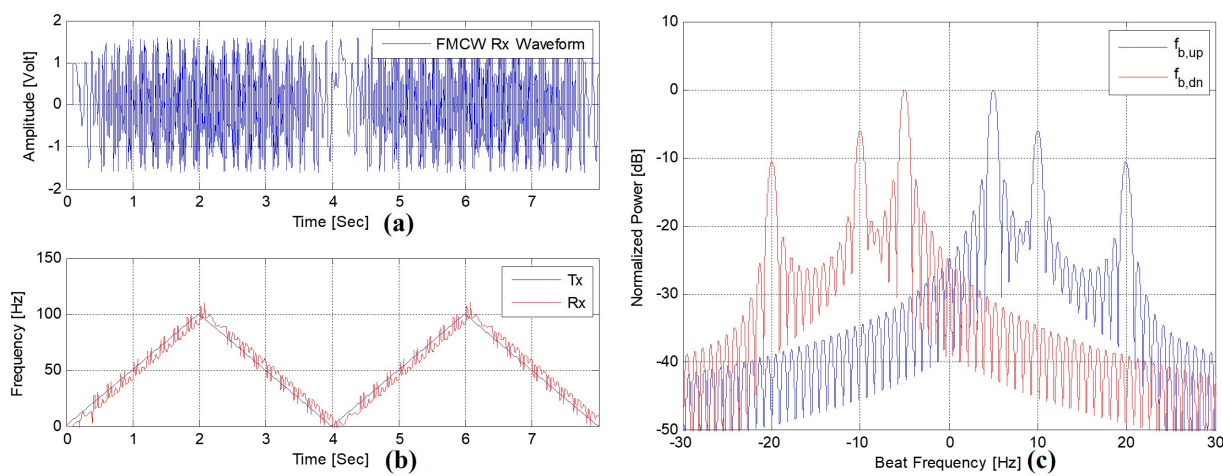


Figure 3. Time and Frequency Domains of Multiple Stationary Targets Signal: (a,b) Time Domains Signal; (c) Frequency Domains Spectrum.

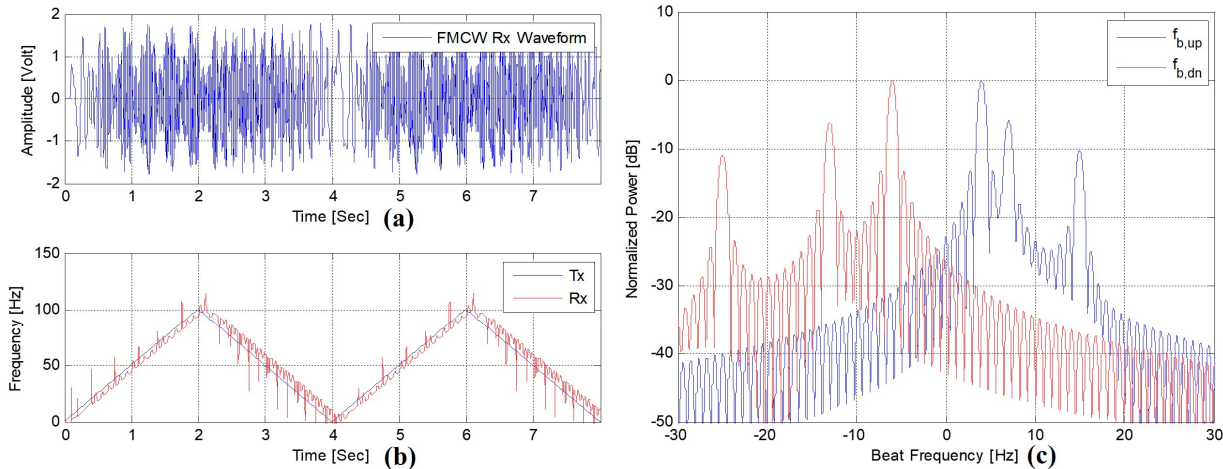


Figure 4. Time and Frequency Domains of Multiple Moving Targets Signal: (a,b)Time Domains Signal; (c) Frequency Domains Spectrum.

3. Tracking System Algorithm

3.1. Target Tracking Procedure

Target tracking is a core technology in BDS radar systems. Figure 5 shows the basic block diagram for target tracking, while Figure 6 depicts the condition of gating algorithm.

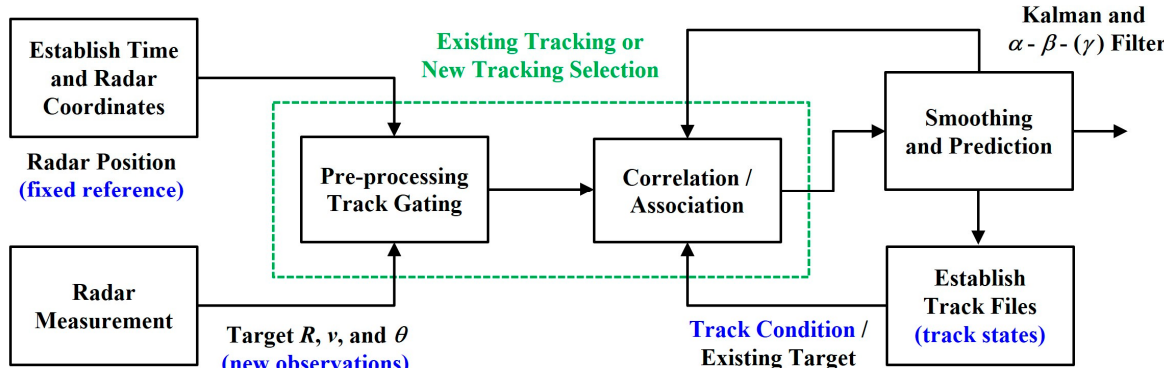


Figure 5. Block Diagram of Target Tracking Processor.

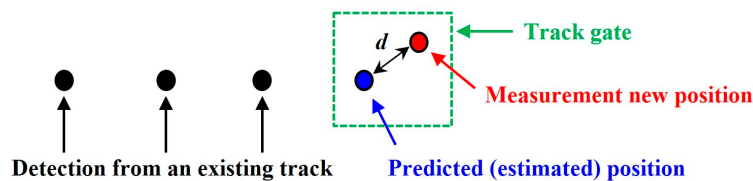


Figure 6. Condition of Gating Algorithm.

A suitable tracking radar system must adopt a fixed reference frame of an inertial coordinate system. The radar measurements consist of target range, velocity, and angle. Gating is used to determine whether an observation is assigned to an existing track file or a new track file. The gating algorithm is based on computing the error distance (d) between the measured and estimated data.

If the error distance (d) is less than the maximum d value of a given track, the observation is said to be correlated with the existing track file. If the new observation does not correlate with any existing tracks, a new track file is established accordingly. If target association is successful, the track files are updated with the new target detection data. Figure 7 illustrates the processor for target tracking in radar signal processing and the operation of the radar system using the data values derived from target tracking. After deriving new R , V , and A data using Radar Measurement, the data are processed using the Target Tracking Scenario set in the system. The resulting data are then passed from the Track Controller to the Radar Sensor Controller, providing information on the current tracking conditions. The provided status information is processed by the Tracking Processor, which generates Track Target Update information that is sent to the Radar System Controller and stored in the radar system's Track History Database.

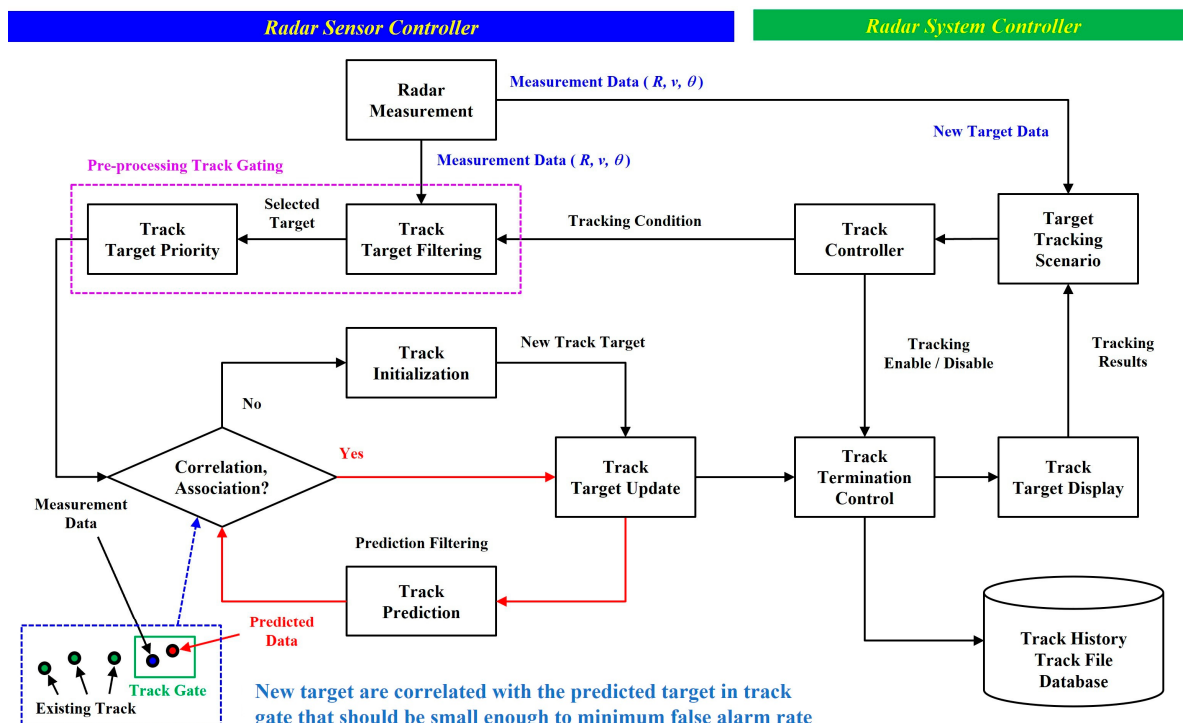


Figure 7. Structure of BSD Radar Tracking Processor.

3.2. Target Filter

In BSD radar, the Kalman filter [24] and the α - β - (γ) filter are commonly used as prediction filters for target tracking. Based on range measurements, the α - β - (γ) filter can predict range, velocity, and constant acceleration. As a fixed gain formulation of

the Kalman filter, it can be easily implemented at low cost, making it primarily used in tracking prediction systems [18]. The α - β filter for range tracking is given by Equations (8)–(10). $r_o(n)$ represents the measured range, $\hat{r}_p(n)$ represents the predicted range at the measurement time, $\hat{r}_s(n)$ represents the smoothed range after the nth observation, $\hat{v}_s(n)$ represents the smoothed velocity after the nth observation, and T_s represents the time between measurements.

Smoothed range is shown as Equation (8):

$$\hat{r}_s(n) = \hat{r}_p(n) + \alpha \cdot [r_o(n) - \hat{r}_p(n)] \quad (8)$$

Smoothed velocity is shown as Equation (9):

$$\hat{v}_s(n) = \hat{v}_s(n-1) + \frac{\beta}{T_s} \cdot [r_o(n) - \hat{r}_p(n)] \quad (9)$$

Predicted range is shown as Equation (10):

$$\hat{r}_p(n+1) = \hat{r}_s(n) + T_s \cdot \hat{v}_s(n) \quad (10)$$

In the equations, the output noise variance of the α - β filter at steady state is minimized when the gain coefficients are related as shown in Equation (11):

$$\beta = \frac{\alpha^2}{(2-\alpha)}, \quad 0 < \alpha < 1 \quad (11)$$

For range and velocity tracking in a system, the α - β - γ filter can be defined by the following equations.

Smoothed range is shown as Equation (12):

$$\hat{r}_s(n) = \hat{r}_p(n) + \alpha \cdot [r_o(n) - \hat{r}_p(n)] \quad (12)$$

Predicted velocity is shown as Equation (13):

$$\hat{v}_s(n) = \hat{v}_s(n-1) + T_s \cdot a_s(n-1) + \frac{\beta}{T_s} \cdot [r_o(n) - \hat{r}_p(n)] \quad (13)$$

Smoothed acceleration is shown as Equation (14):

$$\hat{a}_s(n) = \hat{a}_s(n-1) + \frac{2 \cdot \gamma}{T_s^2} \cdot [r_o(n) - \hat{r}_p(n)] \quad (14)$$

Predicted range is shown as Equation (15):

$$\hat{r}_p(n+1) = \hat{r}_s(n) + T_s \cdot \hat{v}_s(n) + \frac{T_s^2}{2} \cdot \hat{a}_s(n) \quad (15)$$

The gain coefficients are defined as below:

$$\begin{cases} \alpha = 1 - \mu^3 \\ \beta = 1.5 \cdot (1 - \mu^2) \cdot (1 + \mu) \\ \gamma = (1 - \mu)^3 \\ 0 < \mu < 1 \end{cases} \quad (16)$$

Significant smoothing occurs when the value of μ approaches 1, while no smoothing is applied when the value of μ is 0. Figure 8 illustrates the structure of the α - β tracking filter and the α - β - γ filter using the equations described earlier.

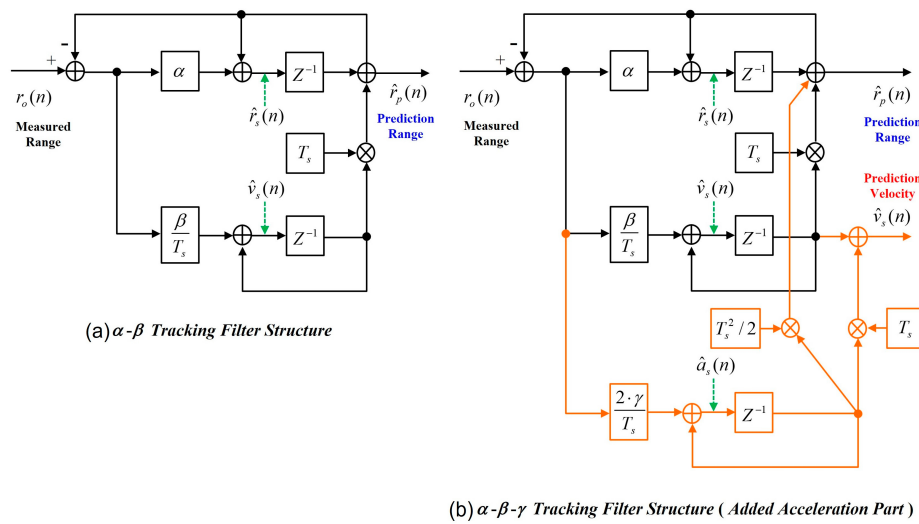


Figure 8. Structure of Tracking Filter; (a) α - β Tracking Filter; (b) α - β - γ Tracking Filter.

4. BSD Radar System Design

4.1. System Architecture

This paper presents the design of antennas operating in the 77 GHz and 79 GHz frequency bands for use in the BSD radar system, and the development of a processing modem and Graphical User Interface (GUI) for radar signal processing. The designed system was integrated into a vehicle to verify the performance of the BSD radar. Figure 9 shows a block diagram of the BSD radar system designed in this paper. The signal input through the four channels undergoes ADC conversion and is then subjected to a windowing process for 1D FFT. The windowing process narrows the main lobe as much as possible to enhance the clarity of the spectrum and minimize the size of minor and side lobes. After performing 1D FFT, 2D Windowing and 2D FFT are executed. Through the process of performing 2D FFT [19–21], Angle Detector information, as well as information for Target Sorting, is provided simultaneously. Then, RDM mapping and 2D Peak Detector are performed. The Binary Detector (3/4) provides binary data to Target Sorting and performs Target Tracking to extract data, which are then used to operate the Warning Logic. Afterwards, the system is configured to operate the BSD radar using Controller Area Network (CAN) communication and GUI.

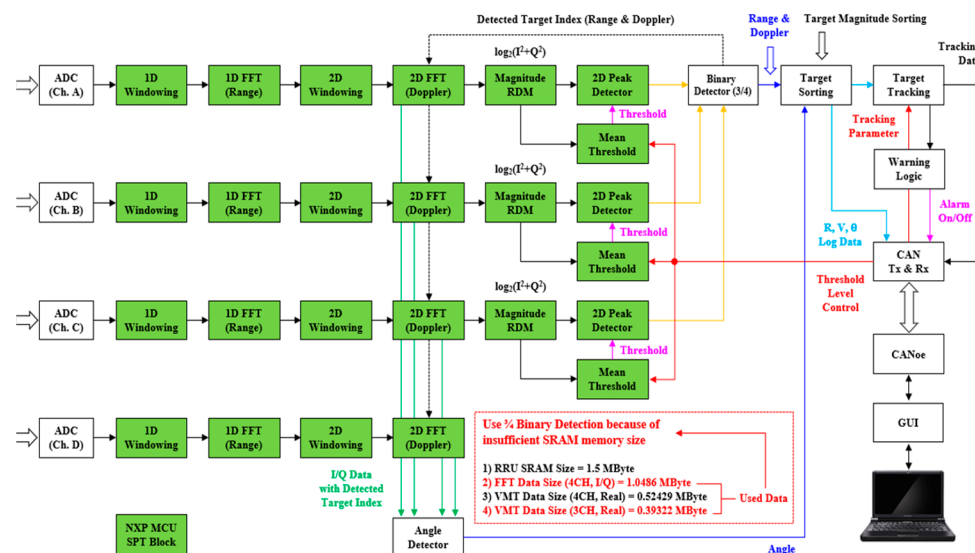


Figure 9. Block Diagram of BSD Radar System.

4.2. System Specification

The system parameters for designing the BSD radar system can be determined based on the detection range, manufacturer's specifications, and radar performance. However, the definition of system parameters refers to the values defined in international standards and standards of each country. Table 3 shows the system parameters for the BSD radar designed in this paper, which were defined to meet the specifications of KS X ISO 17387 [22] and BS ISO 17387 [23]. Table 3 defines the system operating frequency, Tx Antenna Gain (G_t), and Tx Power (P_t) as design conditions. Additionally, it requires Rx Antenna Gain (G_r) for detecting received signals. The table also outlines the size of the FFT used in system design, along with parameters for evaluating system performance, such as System Gain (G_{SYS}), Noise Figure (NF), System Loss (L_{SYS}), and Processing Loss (L_{PRO}). As the detection range (R) is a crucial factor in the performance of BSD radar, BSD radar systems should be designed to meet all the parameters specified in Table 3.

Table 3. Parameters for BSD Radar System.

Parameter	Value	Remark
Operation Frequency	76.5 GHz	Center Frequency
Tx Power (P_t)	10 dBm	
Tx Antenna Gain (G_t)	7 dBi	Antenna Peak Gain (Az.0°)
Rx Antenna Gain (G_r)	12 dBi	Antenna Peak Gain (Az.0°)
Target RCS (σ)		CAR Average RCS
1D FFT Point (N)	256	
2D FFT Point (M)	256	
System Gain (G_{SYS})	3 dB	LNA, LO Gain, etc.
Detection Range (R)	1 m~6 m	
Noise Figure (NF)	15 dB	
System Loss (L_{SYS})	3 dB	Feedline, Mismatch, etc.
System Noise Offset (N_{OFF})	6 dB	System Noise Level Offset
Processing Loss (L_{PRO})	6 dB	Window, Straddle, etc.

Table 4 shows the system parameters required to satisfy the Tx and Rx characteristics of the BSD radar system designed in this paper, while Table 5 shows the parameters required to satisfy the radar system's performance.

Table 4. Parameters for Tx and Rx of BSD Radar System.

Parameter	Value	Unit	Remark
Tx	Center Frequency	GHz	
	Start Frequency	GHz	
	Stop Frequency	GHz	- 76~78 GHz: 10~13 dBm
	Tx Power	dBm	- 78~81 GHz: 7~13 dBm
Rx	Rx Gain	dB	- Rx Gain: 27~45 dB
	High Pass Filter	KHz	- HPF (6 dB): 100~1600 KHz - (100/200/300/400/800/1600)
	Low Pass Filter	MHz	- LPF (6 dB): 7.5~15 MHz - (7.5/10/12.5/15)

Table 4 outlines the parameters necessary for evaluating the performance of the BSD radar system in terms of signal transmission and reception. The Tx system parameters comprise Center Frequency, Start Frequency, Stop Frequency, and Tx Power, which is a critical factor in signal transmission. The Rx system design specifies Rx Gain as a key parameter that can significantly influence receiver performance. Moreover, the frequencies of the High Pass Filter and Low Pass Filter, which are utilized to differentiate between high and low frequencies of the received signal, are defined.

Table 5. Parameters for BSD Radar System Performance.

Parameter	Value	Unit	Remark
Range Detection	64.34	m	Min~Max Range
Range Accuracy	0.5	m	
Range Resolution	0.5	m	
Velocity Detection	± 187	Km/h	Min~Max Range (\pm)
Velocity Accuracy	1.46	Km/h	
Velocity Resolution	1.46	Km/h	
Azimuth Angle (FOV)	± 75	Deg.	Min~Max Range (\pm)
Update Time	25	msec	

Table 5 specifies the performance requirements for the BSD radar system designed to satisfy the criteria outlined in Tables 3 and 4. To interpret the Rx signal reflected by the target from the Tx signal, Detection, Accuracy, and Resolution metrics are defined for both distance and velocity. Azimuth Angle is also defined to determine the range of the BSD, while periodically updating signal analysis results at predefined intervals.

The BSD radar system designed in this paper was developed to meet the radar performance within standardized specifications.

4.3. System Design

The antenna design for transmitting and receiving signals in the BSD radar system must meet the conditions specified in Table 6. The antenna design was developed to meet the requirements of the BSD radar system, considering both the 77 GHz and 79 GHz frequency bands. The system was manufactured using the 77 GHz antenna.

Table 6. Requirements for Antenna Design.

Antenna Type	Parameter	Value	Remark
Tx Antenna	Signal Bandwidth	300 MHz	
	Antenna Beamwidth (3 dB)	Az. $\pm 40^\circ$ /El. $\pm 2.5^\circ$	
	Antenna Gain (3 dB)	15 dBi	
Rx Antenna	1st Sidelobe Level	20 dBc	
	Antenna Beamwidth (3 dB)	Az. $\pm 40^\circ$ /El. $\pm 2.5^\circ$	
	Antenna Gain (3 dB)	15 dBi	
	1st Sidelobe Level	20 dBc	
	Antenna Distance Ratio	$d_{12}: d_{13} = 1.0:2.5$	
	VSWR	2.5:1	

Table 6 outlines the parameters necessary for designing the antennas utilized in the BSD radar system. The Tx antenna must conform to specific Signal Bandwidth and Antenna Beamwidth metrics, in addition to Antenna Gain and Sidelobe Level. Similarly, the Rx antenna must meet the designated Antenna Beamwidth, Antenna Gain, and Sidelobe Level metrics, as well as Antenna Distance Ratio and VSWR. Figures 10 and 11 show antennas that have been designed to meet the specified antenna performance requirements as outlined in Table 6.

Figure 10 shows an antenna for signal processing at 77 GHz, which comprises three Tx array antennas and four Rx array antennas. It has been designed with a center frequency of 76.5 GHz. The antenna distance has been designed to be 1.0λ , 0.5λ , and 0.25λ , with the feedline parameters having a length of 2.5 mm for the microstrip line (1.0λ) and 2.64 mm for the balanced line (1.0λ). The Rx Balun λ parameters have been designed as follows: Rx1: -0.5 , Rx2: Basis; Rx3: -Basis; and Rx4: -0.5 . The Tx Balun λ parameters have been designed as follows: Tx1 (MRR): 0; Tx2 (SRR1): Basis; and Tx3 (SRR2): -0.5 . The Rx and Tx antenna microstrip lengths and λ have been designed as follows: Rx1: 6.9192 mm (1.5λ); Rx2: 3.1692 mm (Basis); Rx3: 4.4192 mm ($+0.5\lambda$); and Rx4: 5.6692 mm ($+1.0\lambda$) for the

Rx antennas, and Tx1: 2.7697 mm ($+0.5 \lambda$); Tx2: 1.5197 mm (Basis); and Tx3: 5.2697 mm ($+1.5 \lambda$) for the Tx antennas.

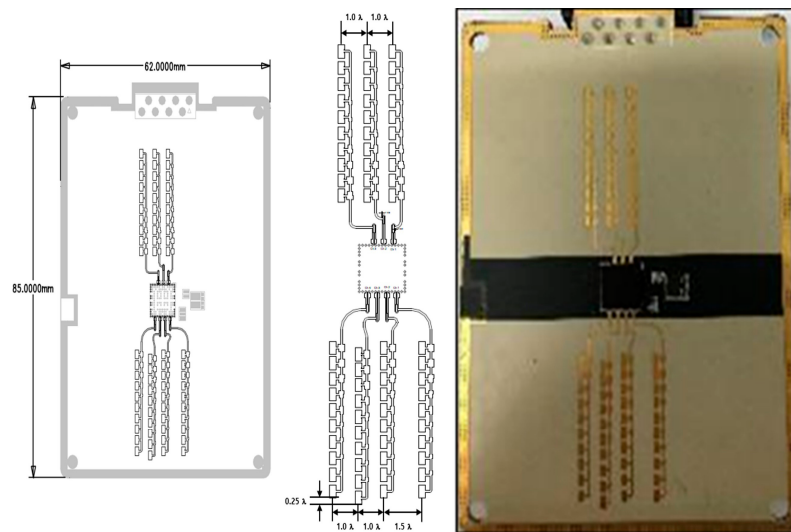


Figure 10. Fabrication of BSD Radar 77 GHz Wide-angle Antenna.

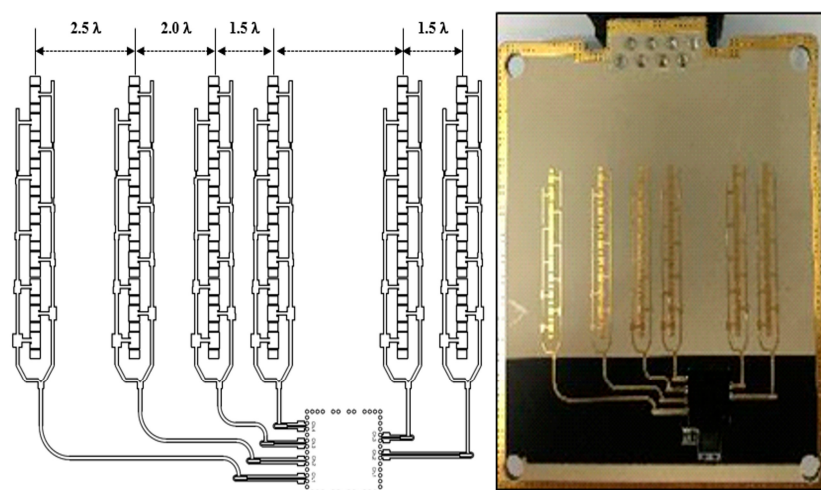


Figure 11. Fabrication of BSD Radar 79 GHz Wide-angle Antenna.

Figure 11 illustrates an antenna for signal processing at 79 GHz, comprising of two Tx array antennas and four Rx array antennas. It has been designed with a center frequency of 78.5 GHz. For the Rx design of the 79 GHz antenna, the microstrip length has been designed as follows: Rx1: 23.6 mm ($+9 \lambda$); Rx2: 14.0001 mm ($+5 \lambda$); Rx3: 6.8 mm ($+2 \lambda$); and Rx4: 2.0 mm (Basis λ). The balanced length has been designed as follows: Rx1: 4.84 mm (1.5λ); Rx2: 3.56 mm ($+1.0 \lambda$); Rx3: 2.28 mm ($+0.5 \lambda$); and Rx4: 1.0 mm (Basis).

To verify the characteristics of the designed antenna, five items related to the basic characteristics of the antenna were tested. Figures 10 and 11 show the pattern and the results of the designed antenna, respectively. Figure 12 shows the result of the BSD radar system produced in this paper. The BSD radar device has been designed with a compact form factor, measuring 7.5 cm \times 6.0 cm \times 2.2 cm (width, length, and height), making it suitable for installation in cars with limited space. The device has been designed for easy insertion into the front and rear corners of the vehicle, ensuring optimal placement for effective operation.

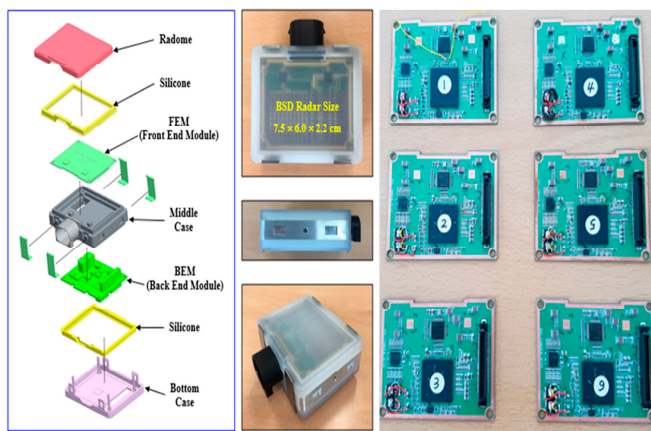


Figure 12. BSD Radar System Design.

5. BSD Radar System Performance Test

This paper proposes a tracking algorithm for the design of a BSD radar system, along with a target tracking procedure and tracking filter to improve system performance. The ultimate objective of this research is to develop a BSD radar system that can operate reliably in real-world driving environments. Therefore, the performance of the designed system is validated in two stages: first, by evaluating the system performance of the produced BSD radar, and second, by assessing the performance of the installed BSD radar system in accordance with the scenarios recommended in ISO 17387.

5.1. Performance Test Configuration

In this paper, a radar system was designed for BSD and installed in a vehicle to perform tests in real road environments. Figure 13 shows the configuration diagram for the performance test of the BSD radar system. A van was used as the test vehicle and four of the designed BSD radars were installed at the back of the vehicle. L1 was installed for left-front detection, L2 for left-rear detection, R1 for right-front detection, and R2 for right-rear detection. Additionally, cameras were installed on the left and right sides of the vehicle's front to monitor the approach and situation of surrounding vehicles. A GUI was developed and installed on a laptop to analyze the data from the performance test and confirm the performance of the BSD radar according to the driving conditions. Data transmission and reception were conducted using the CAN interface. Figure 14 shows the installation of the test vehicle for the performance test.

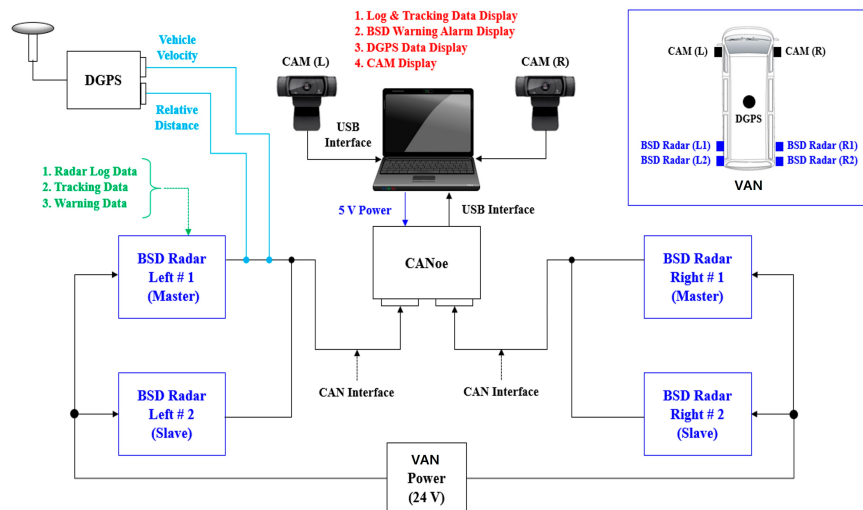


Figure 13. Configuration Diagram for BSD Radar System Performance Test.

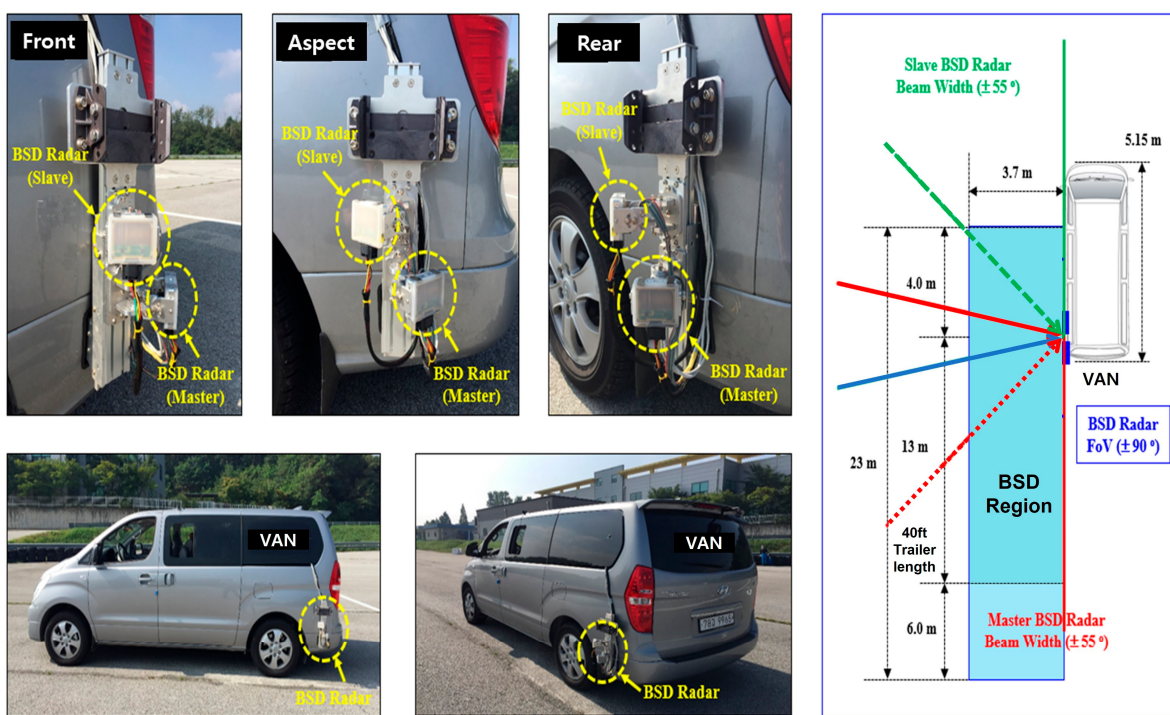


Figure 14. Geometry of BSD Radar Installation and Warning Area.

5.2. Designed BSD Radar Performance

The performance of the BSD radar system was verified using a target simulator for BSD detection during vehicle operation. The evaluation criteria included the maximum detection range, maximum detection speed, response time, maximum detection angle, and distance resolution. The testing methodology for each criterion is described below.

- Maximum detection range: The simulator was set up at distances of 50 m, 52 m, and 55 m to simulate the distance of a forward vehicle. A passenger car size of 10 m^2 was assumed as the target size. The results were compared with the simulation distance to verify whether the detection accuracy was within $\pm 0.5 \text{ mm}$.
- Maximum detection speed: The target simulator was set up with a forward vehicle at a distance of 50 m, driving at speeds of 130 km/h, 140 km/h, and 150 km/h. The target size was assumed to be a passenger car with a size of 10 m^2 . The results were compared with the simulation speed to verify whether the detection accuracy was within $\pm 1 \text{ km/h}$.
- Response time: The target simulator was set up with a forward vehicle at a distance of 50 m, driving at a speed of 100 km/h. The target size was assumed to be a passenger car with a size of 10 m^2 . The results were compared with the target detection response time to verify whether the detection occurred within 50 ms.
- Maximum detection angle: A 10 m^2 corner reflector for vehicle modeling was installed at points corresponding to $\pm 75^\circ$ in the left and right directions. The results were compared with the sensor detection angle to verify whether the detection accuracy was within $\pm 5^\circ$.
- Distance resolution: Two 10 m^2 corner reflectors for vehicle modeling were installed at a distance of 1.5 m apart in the forward and backward directions. The results were compared with the sensor detection distance to confirm the distance resolution (1.5 m).

The performance test results for the five items of the designed BSD radar showed that the maximum detection distance was 55 m, the maximum detection speed was 150 km/h, the response time was 34.64 ms, the maximum detection angle was 150° , and the distance resolution was 1.5 m. The results indicate that the BSD radar installed in the vehicle can meet the performance requirements for ensuring a safe and stable driving environment.

5.3. Performance Test Requirements

The performance test of the designed BSD radar is validated by accurately issuing danger warnings to the driver when a target vehicle enters the BSD area of the radar installed on the test vehicle in real-world road situations. Therefore, danger warning scenarios for the performance test can be defined longitudinally and laterally based on the vehicle's driving and lane-changing in actual road conditions. The warning scenarios can be set using two different cases. Figure 15 shows a conceptual diagram to explain the BSD radar warning scenarios. Using this, the scenarios were defined in accordance with the ISO 17387 standard for BSD radar specifications.

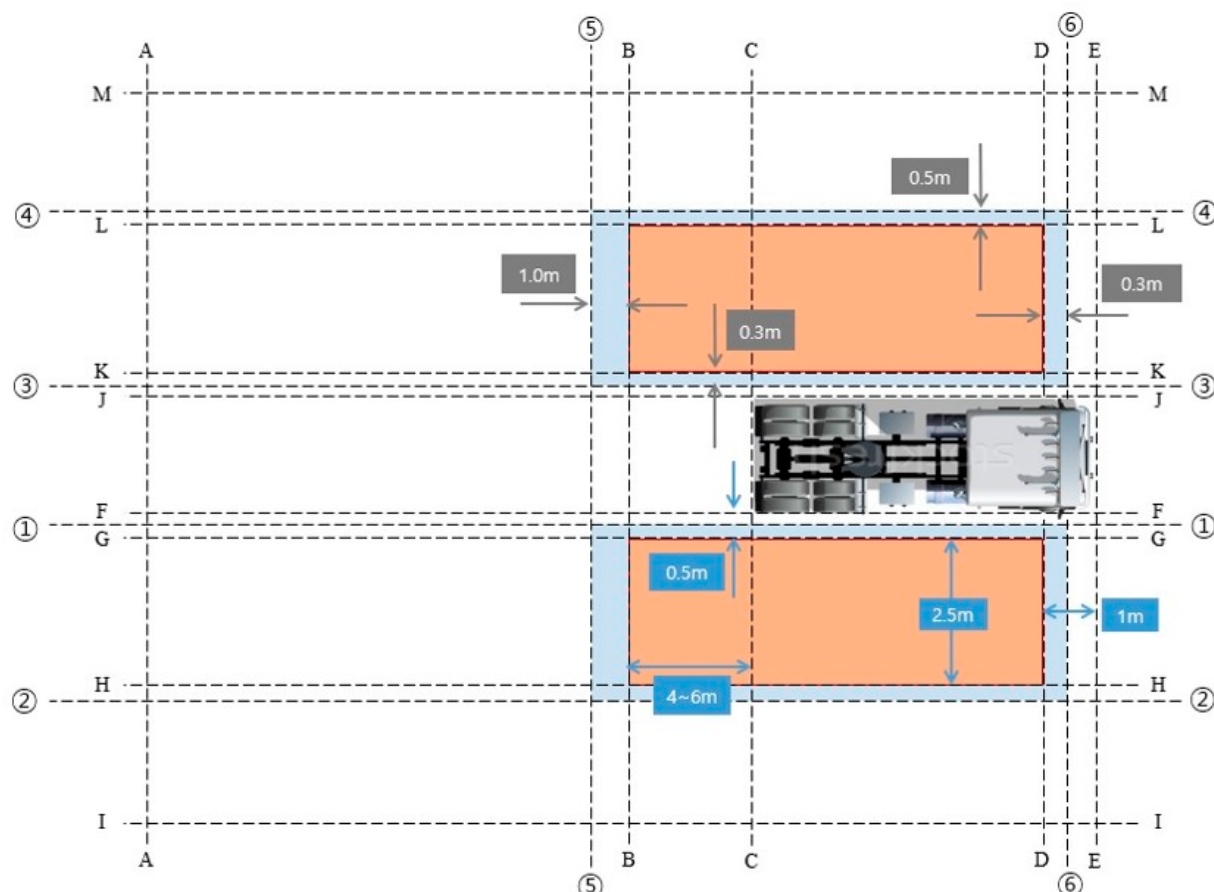


Figure 15. Conceptual Diagram for BSD Radar Warning Scenarios.

Case 1. Longitudinal detection performance test

- Target vehicle overtaking test vehicle
 - The warning should not be activated while the target vehicle is behind Line A.
 - The warning display should be activated within 500 ms after the front of the target vehicle passes Line B.
 - The warning display should be maintained from the moment the front of the target vehicle passes Line B until the rear of the target vehicle completely exits Line ⑥.
 - The warning display should be deactivated within 1 s after the rear of the target vehicle completely exits Line ⑥.
- Test vehicle overtaking target vehicle
 - The warning should not be activated while the target vehicle is behind Line E.

- The warning display should be activated within 500 ms after the front of the target vehicle passes Line D.
- The warning display should be maintained from the moment the front of the target vehicle passes Line D until the rear of the target vehicle completely exits Line ⑤.

Case 2. Lateral detection performance test

- a. Target vehicle driving from left to right
 - The warning should not be activated until the target vehicle is completely positioned to the left of Line M.
 - The left warning display should be activated within 500 ms after the right end of the target vehicle passes Line L.
 - The warning display should be maintained from the moment the right end of the target vehicle passes Line L until the left end of the target vehicle completely passes Line ③.
 - The left warning display should be deactivated within 1 s after the left end of the target vehicle completely passes Line ③.
 - When the warning is deactivated, the system should not issue a warning while the target vehicle is positioned between Line K and Line G.
 - The warning display should be maintained from the moment the right end of the target vehicle passes Line G until the left end of the target vehicle completely passes Line ②.
 - The right warning display should be deactivated within 1 s after the left end of the target vehicle completely passes Line ②.
- b. Target vehicle driving from right to left
 - The warning should not be activated until the target vehicle is completely to the right of Line I.
 - The right warning display should be activated within 500 ms after the left end of the target vehicle passes Line H.
 - The warning display should be maintained from the moment the left end of the target vehicle passes Line H until the right end of the target vehicle completely passes Line ①.
 - The left warning display should be deactivated within 1 s after the right end of the target vehicle completely passes Line ①.
 - When the warning is deactivated, the system should not issue a warning while the target vehicle is positioned between Line K and Line G.
 - The left warning display should be activated within 500 ms after the left end of the target vehicle passes Line K.
 - The warning display should be maintained from the moment the left end of the target vehicle passes Line K until the right end of the target vehicle completely passes Line ④.
 - The left warning display should be deactivated within 1 s after the right end of the target vehicle completely passes Line ④.

5.4. Performance Evaluation

This paper described the design of a BSD radar system and validated its performance by proposing five performance test scenarios that consider the driving environment of the vehicle. The operation of the BSD radar was verified in the proposed driving environments, and the scenarios were written in accordance with the ISO 17387 standard for the BSD radar specifications.

Case 1. BSD longitudinal detection performance evaluation, target vehicle overtaking test vehicle:

- a. The test vehicle drives at a constant speed of 40 kph, while the target vehicle approaches from behind at a constant speed of 45 kph and overtakes the test vehicle.

The longitudinal distance of the target vehicle is measured based on the timing of when the warning was turned ON or OFF.

- b. Warning ON: The moment when the front of the target vehicle enters the BSD area.
- c. Warning OFF: The moment when the rear of the target vehicle exits the BSD area.

Case 2. BSD longitudinal detection performance evaluation, test vehicle overtaking target vehicle:

- a. The target vehicle drives at a constant speed of 35 kph, while the test vehicle approaches from behind at a constant speed of 40 kph and overtakes the target vehicle. The longitudinal distance of the target vehicle is measured based on the timing of when the warning is turned ON or OFF.
- b. Warning ON: The moment when the rear of the target vehicle enters the BSD area.
- c. Warning OFF: The moment when the front of the target vehicle exits the BSD area.

Case 3. BSD lateral detection performance evaluation, target vehicle changing lanes laterally:

- a. The test vehicle drives at a constant speed of 40 kph, while the target vehicle changes lanes from the adjacent lane to the next lane at the same speed. The distance of the target vehicle is measured based on the timing of when the warning is turned ON or OFF.
- b. Warning ON: The moment when the inner side of the target vehicle relative to the test vehicle enters the BSD area.
- c. Warning OFF: The moment when the inner side of the target vehicle relative to the test vehicle exits the BSD area.

Case 4. Cyclist detection performance evaluation, cyclist approaching test vehicle:

- a. The test vehicle drives at a constant speed of 10 kph and the distance is measured when a cyclist approaches the BSD area of the test vehicle.
- b. Warning ON: The moment when the cyclist enters the BSD area.
- c. Warning OFF: The moment when the cyclist exits the BSD area.

Case 5. Pedestrian detection performance evaluation, pedestrian approaching test vehicle:

- a. The test vehicle drives at a constant speed of 10 kph and the distance is measured when a pedestrian approaches the BSD area of the test vehicle.
- b. Warning ON: The moment when the pedestrian enters the BSD area.
- c. Warning OFF: The moment when the pedestrian exits the BSD area.

5.5. Results

In order to evaluate the performance of the BSD radar, a testing environment was created, and the radar was installed on a vehicle to verify its performance in real-world road environments. To conduct the performance tests, five test scenarios were presented in accordance with the BSD radar specifications and its performance was evaluated under actual road conditions.

In Case 1, as a test of target vehicle overtaking test vehicle, the test vehicle drove at a constant speed of 40 kph while the target vehicle approached from behind at a constant speed of 45 kph and overtook the test vehicle. The longitudinal distance of the target vehicle was measured based on the timing of when the warning was turned ON or OFF. As shown in Figure 16, the warning was activated when the target vehicle entered the BSD area of the test vehicle. The warning was deactivated when it exited the BSD area.

In Case 2, as a test of test vehicle overtaking target vehicle, the target vehicle drove at a constant speed of 35 kph while the test vehicle approached from behind at a constant speed of 40 kph and overtook the target vehicle. The longitudinal distance of the target vehicle was measured based on the timing of when the warning was turned ON or OFF. As shown in Figure 17, the warning was activated when the target vehicle entered the BSD

area of the test vehicle as the test vehicle approached it for overtaking. The warning was deactivated when the target vehicle passed the test vehicle and exited the BSD area.

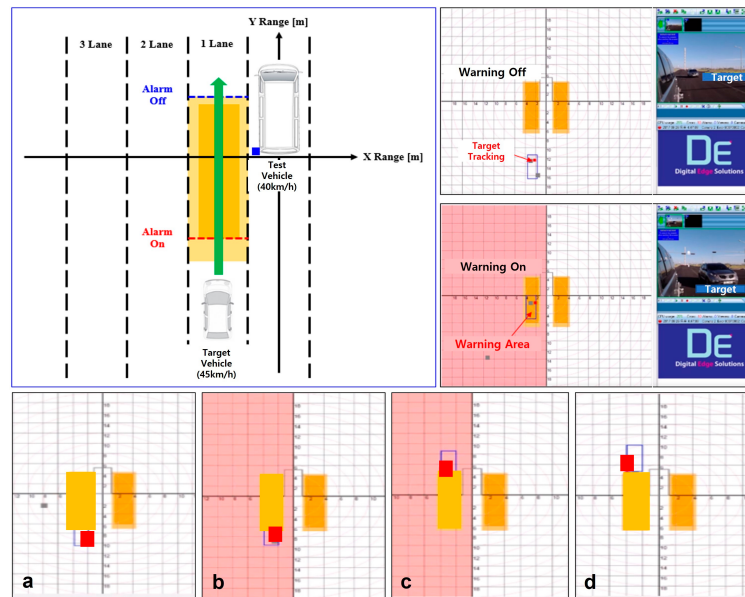


Figure 16. Test Operation Scenarios and Results of Target Vehicle Overtaking Test Vehicle: (a) Before the target vehicle enters the BSD area of the test vehicle; (b) When the target vehicle enters the BSD area of the test vehicle (Warning ON); (c) Before the target vehicle exits the BSD area of the test vehicle; (d) When the target vehicle exits the BSD area of the test vehicle (Warning OFF).

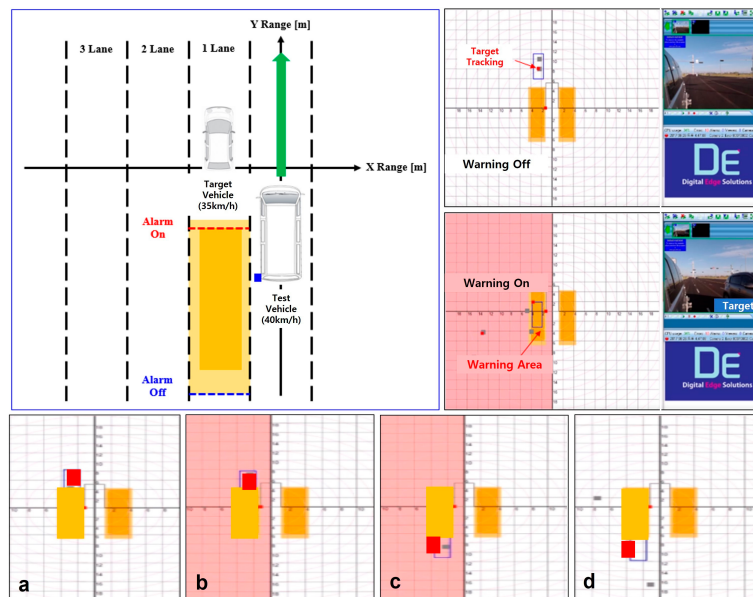


Figure 17. Test Operation Scenarios and Results of Test Vehicle Overtaking Target Vehicle: (a) Before the target vehicle enters the BSD area of the test vehicle; (b) When the target vehicle enters the BSD area of the test vehicle (Warning ON); (c) Before the target vehicle exits the BSD area of the test vehicle; (d) When the target vehicle exits the BSD area of the test vehicle (Warning OFF).

In Case 3, as a test of target vehicle changing lanes laterally, the test vehicle drove at a constant speed of 40 kph while the target vehicle changed lanes from the adjacent lane to the next lane at the same speed. The distance of the target vehicle was measured based on the timing of when the warning was turned ON or OFF. As shown in Figures 18 and 19,

the warning was activated when the target vehicle entered the BSD area of the test vehicle during the lane change. The warning was deactivated when the target vehicle completed the lane change and exited the BSD area.

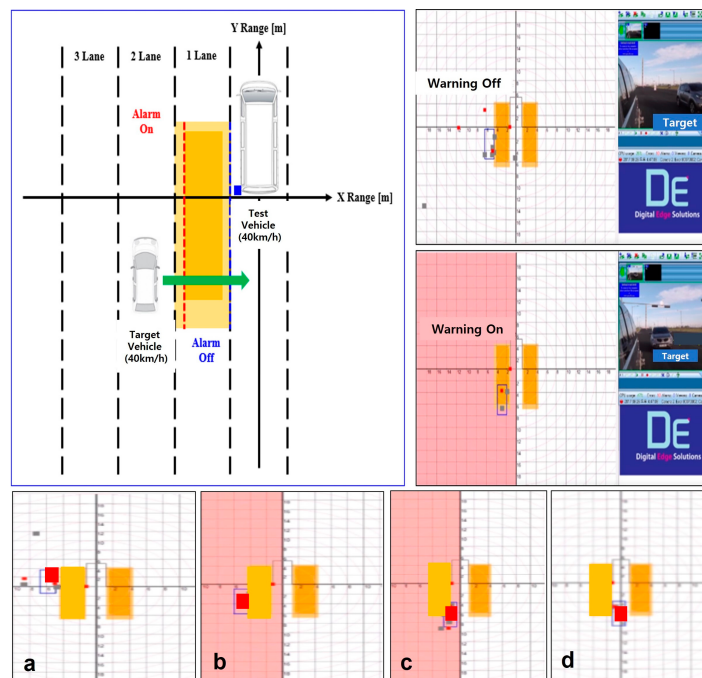


Figure 18. Test Operation Scenarios and Results of Target Vehicle Changing Lanes from Outside to Inside: (a) Before the target vehicle enters the BSD area of the test vehicle; (b) When the target vehicle enters the BSD area of the test vehicle (Warning ON); (c) Before the target vehicle exits the BSD area of the test vehicle; (d) When the target vehicle exits the BSD area of the test vehicle (Warning OFF).

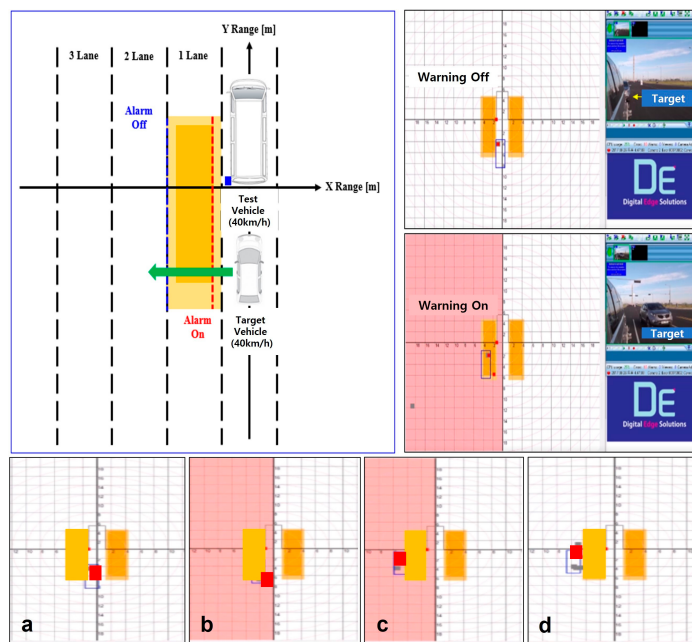


Figure 19. Test Operation Scenarios and Results of Target Vehicle Changing Lanes from Inside to Outside: (a) Before the target vehicle enters the BSD area of the test vehicle; (b) When the target vehicle enters the BSD area of the test vehicle (Warning ON); (c) Before the target vehicle exits the BSD area of the test vehicle; (d) When the target vehicle exits the BSD area of the test vehicle (Warning OFF).

In Case 4, as a test of cyclist approaching test vehicle, the test vehicle drove at a constant speed of 10 kph and the distance was measured when a cyclist approached the BSD area of the test vehicle. As shown in Figure 20, the warning was activated when the cyclist entered the BSD area of the test vehicle. The warning was deactivated when the cyclist exited the BSD area.

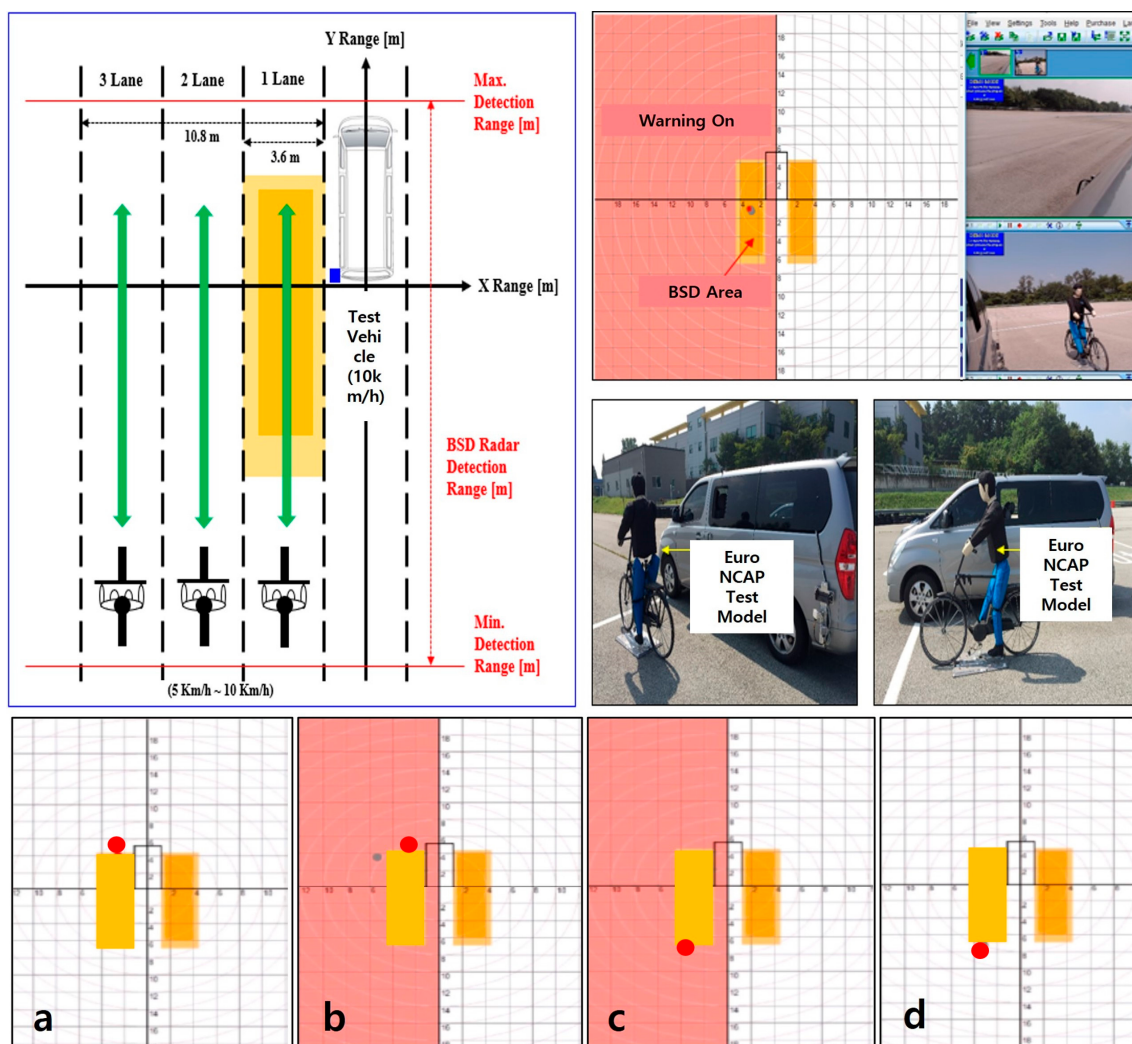


Figure 20. Test Operation Scenarios and Results of Cyclist Approaching Test Vehicle: (a) Before the cyclist enters the BSD area of the test vehicle; (b) When the cyclist enters the BSD area of the test vehicle (Warning ON); (c) Before the cyclist exits the BSD area of the test vehicle; (d) When the cyclist exits the BSD area of the test vehicle (Warning OFF).

In Case 5, as a test of pedestrian approaching test vehicle, the test vehicle drove at a constant speed of 10 kph and the distance was measured when a pedestrian approached the BSD area of the test vehicle. To conduct the test, models of an adult with a height of 180 cm and a child with a height of 120 cm were used. As shown in Figure 21, the warning was activated when the pedestrian entered the BSD area of the test vehicle. The warning was deactivated when the pedestrian exited the BSD area.

The test results confirmed that the warning system of the designed BSD radar operated properly in each of the scenarios. To produce the BSD radar, this paper presented target tracking procedures and tracking algorithms, and fabricated antennas and modems. After installing these in a vehicle, performance tests were conducted, and ideal results were achieved. The BSD radar system developed in this paper is a promising technology.

that can enhance the active safety system of vehicles and support the emergence of fully autonomous driving systems in the future. However, in complex driving environments, determining the priority of multiple target vehicles remains a challenge that requires additional technological advances. Currently, radar systems allocate the same amount of time to detect all target vehicles, which can lead to tracking failures under certain circumstances. To overcome this challenge, incorporating AI technology to determine the priority of target vehicles and allocate different tracking times could improve the accuracy of target tracking. Based on the BSD radar system presented in this paper, we are conducting research on assigning priorities to target vehicles using AI technology.

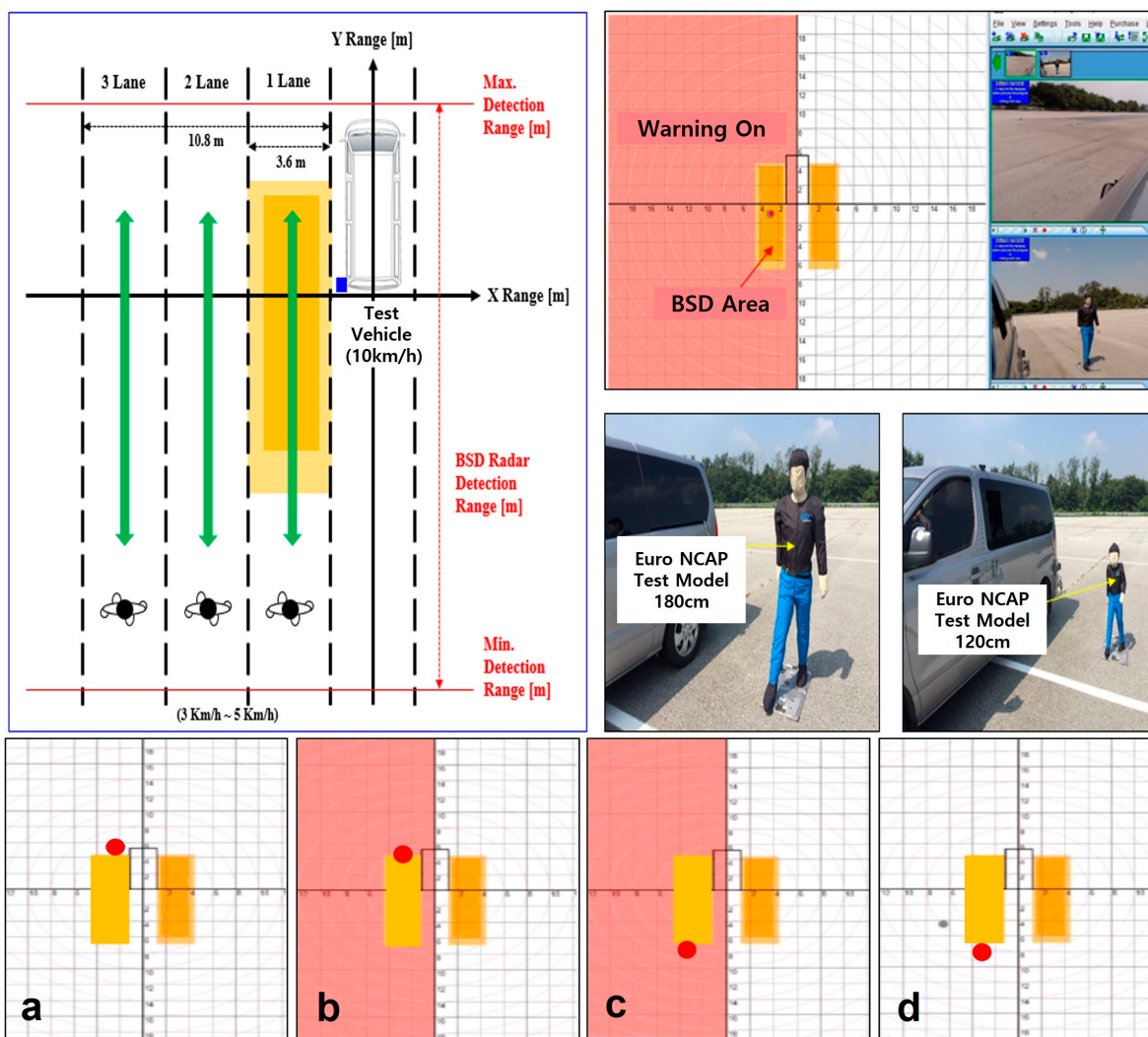


Figure 21. Test Operation Scenarios and Results of Pedestrian Approaching Test Vehicle: (a) Before the pedestrian enters the BSD area of the test vehicle; (b) When the pedestrian enters the BSD area of the test vehicle (Warning ON); (c) Before the pedestrian exits the BSD area of the test vehicle; (d) When the pedestrian exits the BSD area of the test vehicle (Warning OFF).

6. Discussion

In pursuit of this goal, this paper presented the hardware design of the BSD radar system, including antenna and modem designs. Additionally, a tracking algorithm, tracking procedure, and tracking filter were developed for BSD detection. The BDS radar system was verified through GUI design and performance tests based on BSD radar specifications. The performance evaluation showed ideal test results. During the performance testing of the BSD radar system installed on a vehicle, there were instances where the system failed to

track target vehicles due to the high speed of the target or complex driving environments that presented irregular situations. These findings highlight the need for further research to develop a system that can assign priorities to target vehicles based on their threat level and allocate different tracking times accordingly.

As a part of future research, this paper is exploring AI algorithms using Fuzzy Inference to apply AI technology to the BSD radar system designed in this paper. The goal is to design a BSD radar system that incorporates AI technology in the future.

Author Contributions: W.K. is an expert in this field of intelligent vehicle research and conducts various Korea National Projects. H.Y. and W.K. conceived and validated the idea for this paper through simulation, and J.K. contributed to GUI design. All authors conducted experiments using the BSD radar system, contributed to the construction of the BSD radar system, and J.K. edited the paper. All authors have read and agreed to the published version of the manuscript.

Funding: This research received no external funding.

Institutional Review Board Statement: Not applicable.

Informed Consent Statement: Not applicable.

Data Availability Statement: Not applicable.

Conflicts of Interest: The authors declare no conflict of interest.

References

1. Rindone, C. Sustainable Mobility as a Service: Supply Analysis and Test Cases. *Information* **2022**, *13*, 351. [[CrossRef](#)]
2. Musolino, G.; Rindone, C.; Vitetta, A. Models for Supporting Mobility as a Service (MaaS) Design. *Smart Cities* **2022**, *5*, 206–222. [[CrossRef](#)]
3. Battaglia, G.; Musolino, G.; Vitetta, A. Freight Demand Distribution in a Suburban Area: Calibration of an Acquisition Model with Floating Car Data. *J. Adv. Transp.* **2022**, *2022*, 1535090. [[CrossRef](#)]
4. Mouftah, H.T.; Erol-Kantarci, M.; Sorour, S. (Eds.) *Connected and Autonomous Vehicles in Smart Cities*; CRC Press: Boca Raton, FL, USA, 2020.
5. Cafiso, S.; Pappalardo, G. Safety effectiveness and performance of lane support systems for driving assistance and automation—Experimental test and logistic regression for rare events. *Accid. Anal. Prev.* **2020**, *148*, 105791. [[CrossRef](#)] [[PubMed](#)]
6. Dai, W.; Pan, Y.; Min, C.; Zhang, S.P.; Zhao, J. Real-Time Modeling of Vehicle's Longitudinal-Vertical Dynamics in ADAS Applications. *Actuators* **2022**, *11*, 378. [[CrossRef](#)]
7. Pak, J.M. Hybrid Interacting Multiple Model Filtering for Improving the Reliability of Radar-Based Forward Collision Warning Systems. *Sensors* **2022**, *22*, 875. [[CrossRef](#)] [[PubMed](#)]
8. Andrei, M.A.; Boiangiu, C.A.; Tarbă, N.; Voncila, M.L. Robust Lane Detection and Tracking Algorithm for Steering Assist Systems. *Machines* **2022**, *10*, 10. [[CrossRef](#)]
9. Lee, Y.W.; Kim, T.W.; Kim, J.G.; Kang, Y. Vehicle and Pedestrian Classification Using 24 GHz Radar for Vehicle Rear Cross-Traffic Alert Systems. *J. Inst. Control. Robot. Syst.* **2018**, *3*, 247–255. [[CrossRef](#)]
10. Yang, J.; Jiang, D.; Tao, J.; Gao, Y.; Lu, X.; Han, Y.; Liu, M. A Sector-Matching Probability Hypothesis Density Filter for Radar Multiple Target Tracking. *Appl. Sci.* **2023**, *13*, 2834. [[CrossRef](#)]
11. Richards, M.A. *Fundamentals of Radar Signal Processing*; Tata McGraw-Hill Education: New York, NY, USA, 2005.
12. Stove, A.G. Linear FMCW radar techniques. *IEE Proc. Rad. Sig. Process.* **1992**, *139*, 343–350. [[CrossRef](#)]
13. Kim, B.; Kim, S.; Jin, Y.; Lee, J. High-Efficiency Super-Resolution FMCW Radar Algorithm Based on FFT Estimation. *Sensors* **2021**, *12*, 4018. [[CrossRef](#)] [[PubMed](#)]
14. Rohling, H. Radar CFAR Thresholding in Clutter and Multiple Target Situations. *IEEE Trans. Aerosp. Electron. Syst.* **1983**, *AES-19*, 608–621. [[CrossRef](#)]
15. Barniv, Y. Dynamic programming solution for detecting dim moving targets. *IEEE Trans. Aerosp. Electron. Syst.* **1985**, *21*, 144–156. [[CrossRef](#)]
16. MATLAB Phased Array System Toolbox Documentation. Available online: <https://www.mathworks.com/help/phased> (accessed on 7 April 2021).
17. Mahafza, B.R. *Radar Systems Analysis and Design Using MATLAB*; Chapman and Hall/CRC: Boca Raton, FL, USA, 2005.
18. Zhang, H.; Yang, Z.; Xiong, H.; Zhu, T.; Long, Z.; Wu, W. Transformer Aided Adaptive Extended Kalman Filter for Autonomous Vehicle Mass Estimation. *Processes* **2023**, *11*, 887. [[CrossRef](#)]
19. Hyun, E.; Jin, Y.; Lee, J. A pedestrian detection scheme using a coherent phase difference method based on 2D range-Doppler FMCW radar. *Sensors* **2016**, *16*, 124. [[CrossRef](#)] [[PubMed](#)]
20. Feng, X.; Zhao, Z.; Li, F.; Cui, W.; Zhao, Y. Radar Phase-Coded Waveform Design with Local Low Range Sidelobes Based on Particle Swarm-Assisted Projection Optimization. *Remote Sens.* **2022**, *14*, 4186. [[CrossRef](#)]

21. Saponara, S.; Neri, B. Radar sensor signal acquisition and multidimensional FFT processing for surveillance applications in transport systems. *IEEE Trans. Instrum. Meas.* **2017**, *66*, 604–615. [[CrossRef](#)]
22. KS X ISO 17387:2012; Intelligent Transport Systems-Lane Change Decision Aid Systems (LCDAS)—Performance Requirements and Test Procedures. KATS: Maengdong-myeon, Republic of Korea, 2012.
23. BS ISO 17387:2008; Intelligent Transport Systems-Lane Change Decision Aid Systems (LCDAS)—Performance Requirements and Test Procedures. ISO: Geneva, Switzerland, 2008.
24. Yildiz, R.; Barut, M.; Zerdali, E. A comprehensive comparison of extended and unscented kalman filters for speed-sensorless control applications of induction motors. *IEEE Trans. Ind. Inform.* **2020**, *16*, 6423–6432. [[CrossRef](#)]

Disclaimer/Publisher’s Note: The statements, opinions and data contained in all publications are solely those of the individual author(s) and contributor(s) and not of MDPI and/or the editor(s). MDPI and/or the editor(s) disclaim responsibility for any injury to people or property resulting from any ideas, methods, instructions or products referred to in the content.